Separation of hot-electron and self-heating effects in two-dimensional AlGaN/GaN-based conducting channels

S. A. Vitusevich,[a),b)] S. V. Danylyuk,[a)] and N. Klein
Institut für Schichten und Grenzflächen, Forschungszentrum Jülich, Jülich D-52425, Germany

M. V. Petrychuk, A. Yu. Avksentyev, V. N. Sokolov, V. A. Kochelap, and A. E. Belyaev
Institute of Semiconductor Physics, NASU, Kiev 03028, Ukraine

V. Tilak, J. Smart, A. Vertiatchikh, and L. F. Eastman
School of Electrical Engineering, Cornell University, Ithaca, New York 14853

(Received 11 October 2002; accepted 11 December 2002)

We address experimental and theoretical study of a two-dimensional electron gas transport at low and moderate electric fields. The devices under study are group-III nitride-based (AlGaN/GaN) gateless heterostructures grown on sapphire. The transmission line model patterns of different channel lengths, L, and of the same channel width are used. A strong dependence of the device $I-V$ characteristics on the channel length has been found. We have developed a simple theoretical model to adequately describe the observed peculiarities in the $I-V$ characteristics measured in steady-state and pulsed (10^{-6} s) regimes. The effect of the Joule heating of a heterostructure is clearly distinguished. The thermal impedance and the channel temperature rise caused by the Joule self-heating have been extracted for the devices of different L at different values of dissipated power. The current reduction due to both self-heating and hot-electron effects is determined quantitatively as a function of the electric field. © *2003 American Institute of Physics.*
[DOI: 10.1063/1.1542928]

It has been established that at the AlGaN/GaN heterointerface a conducting channel is formed with two-dimensional electron gas (2DEG). A high electron concentration in the channel is achieved without intentional doping due to large polarization fields inherent in the nitride material system.[1] Both experimental and theoretical investigations[2–5] indicate that the electron transport in the conducting channels reveals a number of properties quite different from what has been observed in other III–V heterostructures.

High carrier concentrations (in excess of 10^{13} cm^{-2}) and large values of the electron mobility and operating voltages (dissipative power densities are in a few watts per millimeter range) make it necessary to distinguish hot-electron effect and self-heating phenomena for better understanding transport properties aimed to use the group III-nitride heterostructures in high power and high temperature microelectronic applications.

Indeed, since the carrier mobility is dependent on both electric field strength, E, and lattice temperature, T_0, two effects are present simultaneously: hot electrons[6] and self-heating.[7,8] The self-heating is a local increase in crystal temperature due to dissipated Joule electric power, P_{dis}. Separation between these effects is important to clarify the thermal budget of devices which optimization allows to reach the best device performance. A distinction can be made by studying the change in transport characteristics by varying dissipated power P_{dis} at the same values of the electric field E. In this letter, we realized the separation of hot-electron and self-heating effects by the study of AlGaN/GaN gateless heterostructures [transmission line model (TLM) patterns] with different lengths L of the conducting channel.

The investigated devices are fabricated from AlGaN/GaN (33% Al) undoped heterostructures of 1.1 μm GaN and 23 nm AlGaN covered with a 320 nm Si_3N_4 passivation layer. The TLM structures are patterned on the same wafer as used for high electron mobility transistor (HEMT) device formation grown by metalorganic chemical vapor deposition on sapphire with 40 nm AlGaN (16% Al) intermediate nucleation layer. The conducting channel of devices is of the width $W=100$ μm with the intercontact length L scaled to varied distance as 1, 5, 10, 15, 20, and 25 μm. The TLM ohmic contacts were processed by Ti/Al/Ti/Au metallization annealed for 40 s at 800 °C. A room temperature mobility of 1250 cm^2/V s at a sheet carrier density of 1.05×10^{13} cm^{-2} has been measured in the 2DEG of the channel by means of the Van der Pauw method. The $I-V$ characteristics have been measured in steady-state and transient current conditions with a time sweep as low as 10^{-6} s (Fig. 1). Three different regions are resolved in the $I-V$ characteristics: a low voltage (ohmic) region followed by sublinear and saturation (or negative differential resistance) regions of current. The regime of operation with saturation current for AlGaN/GaN TLM structures has not been reported in literature. Typically the saturation regime arises in HEMT structures as a gate effect. In gateless TLM structures the saturation is of a different origin.

The main results obtained on the electron transport characterization in the TLM AlGaN/GaN heterostructures are presented in Fig. 2 as $I-E$ curves, with $E=V/L$ being an average electric field in the conducting channel. The simple geometry of the gateless devices provides this average field

[a)]On leave from: ISP NAS of Ukraine, Kiev, Ukraine.
[b)]Electronic mail: s.vitusevich@fz-juelich.de

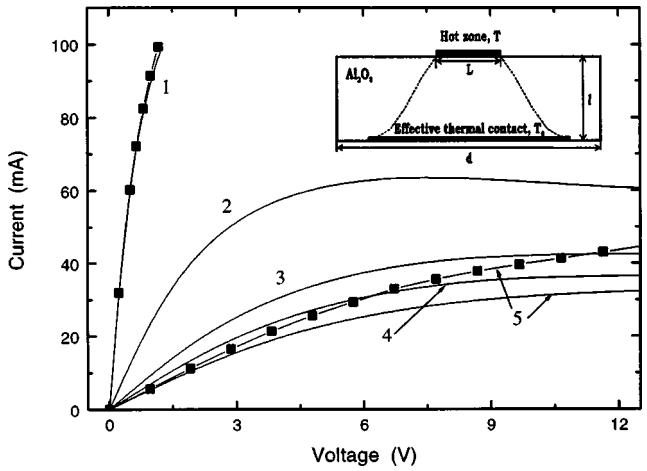

FIG. 1. Current–voltage characteristics of TLM structures measured in steady-state (solid lines) and pulsed (solid squares) regimes for different channel lengths L (μm): 1–1, 2–5, 3–15, 4–20, 5–25. Inset: illustration of considered thermal model.

to coincide with the local electric field in the channel. The resistance of the ohmic region is proportionally scaled down with TLM intercontact distance and shows a good coincidence in $I=f(E)$ dependence. Both pulsed and dc measurements show dependence of the current on the channel length. The longer the channel, the greater the observed difference between dc and pulsed $I-E$ characteristics. With increasing L a portion on the $I-E$ curve with saturation current manifests itself already in the range of measured electric field less than 8 kV/cm. In general, the obtained $I-E$ characteristics are strongly nonlinear although the considered field range ($<$8 kV/cm) is still below the fields of well-developed hot-electron regime expected from theoretical predictions.[3,4]

For a description of the observed behavior of the $I-E$ characteristics we use a simple theoretical model based on (i) heat dissipation and heat-transfer modeling in the device and (ii) self-consistent solution of coupled nonlinear equations for the channel current I and the channel temperature T. The latter is determined by dissipated power $P_{\rm dis}$ and heat conduction properties in the device.

We suppose that corresponding thermal impedance is primarily determined by the sapphire substrate[7] (see the inset in Fig. 1). If we neglect on the first stage of our analysis the temperature dependence in the thermal conductivity of the substrate, $\lambda(T)$, the problem is reduced to the Laplace equation.[9,10] The boundary conditions can be set as a constant heat flux $q=P_{\rm dis}/(WL)$ from hot zone (conducting channel) on the top of the substrate; adiabatic thermal conditions all over the remainding surface ($q=0$), except the bottom where an isothermal condition is provided with a given temperature T_0. These allow us to find temperature distribution in the substrate and evaluate the channel temperature, T, averaged over the channel area, $S_{\rm ch}=WL$. The temperature rise $\Delta T=T-T_0$ in the channel is related to $P_{\rm dis}$ through the chord thermal impedance $\theta=\Delta T/P_{\rm dis}$. The linear one can be written as

$$\theta=l/\lambda S_{\rm eff},\quad S_{\rm eff}=d^2/[1+\sigma(L/d,W/d,l/d)], \tag{1}$$

where the function $\sigma=2(\sigma_1+2\sigma_2)$ is expressed in terms of infinite series[11]

$$\sigma_1=\sum_{n=1}[\varphi_n^2(W/d)+\varphi_n^2(L/d)]\ \psi_{n=m}(l/d\sqrt{2}), \tag{2}$$

$$\sigma_2=\sum_{n,m=1}^{\infty}\varphi_n^2(L/d)\varphi_m^2(W/d)\psi_{nm}(l/d), \tag{3}$$

with $\varphi_n(x)=\sin(n\pi x)/(n\pi x)$ and $\psi_{nm}(x)=\tan(2\pi x\sqrt{n^2+m^2})/(2\pi x\sqrt{n^2+m^2})$. For $L=W=d$, we get $\sigma=0$ and $S_{\rm eff}=S=d^2$. Then Eq. (1) reduces to the thermal impedance under a one-dimensional heat conduction. For $(W,L)<d$, we get $\sigma>0$ and, respectively, $S_{\rm eff}<S$, which leads to an increase in the thermal impedance due to three-dimensional character of the heat conduction.

The current I as a function of electric field E can be determined from coupled equations

$$I=e\mu(T_0+\Delta T,E)NWE, \tag{4}$$

$$\Delta T=\theta(T_0,L,P_{\rm dis})P_{\rm dis}, \tag{5}$$

$$P_{\rm dis}=IEL. \tag{6}$$

Here e is the electron charge, μ is the electron mobility, N is the sheet electron concentration in the conducting channel, $P_{\rm dis}=IEL$. Later numerical solutions to Eqs. (4)–(6) are found taking advantage of the earlier linear and nonlinear thermal impedance,[9] as well as the recent results on the Monte Carlo simulation[4] of the 2D electron transport and experimental study of the low field mobility on temperature at elevated temperatures in nitride heterostructures.[12] Specifically, we take for the field dependence of the electron mobility $\mu(T,E)=\mu_0(T)/[1+\zeta(E/E_c)^{\beta}]$, with β, ζ, and E_c being fitting parameters.[4] The low field electron mobility[12] is taken to be $\mu_0(T)=\mu_{300}(300/T)^{1.8}$, where μ_{300} is the electron mobility at room temperature.

Thus, we have obtained the current I and the temperature rise ΔT as a function of the electric field E in the channels with different lengths L. The results of calculations I vs E for $L=1$ and 25 μm are presented in Fig. 2 compared with the experimental curves. For these calculations we have used the

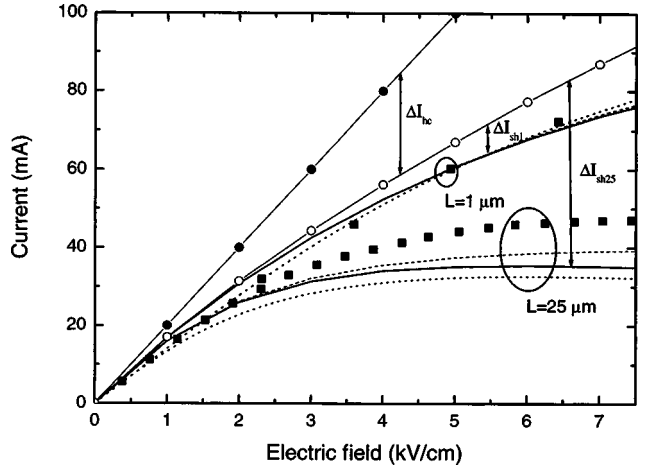

FIG. 2. The result of calculation I vs E for $L=1$ and 25 μm (dashed—linear, solid—nonlinear self-heating) are compared with the experimental results: dc—dotted lines, 1 μs pulse—solid squares. Solid and open circles—calculated ohmic and hot-electron $I-E$ curves. Current reduction due to hot-electron, $\Delta I_{\rm he}$, and self-heating effects for two channel lengths of 1 μm ($\Delta I_{\rm sh1}$), and 25 μm ($\Delta I_{\rm sh25}$) is shown by vertical arrows.

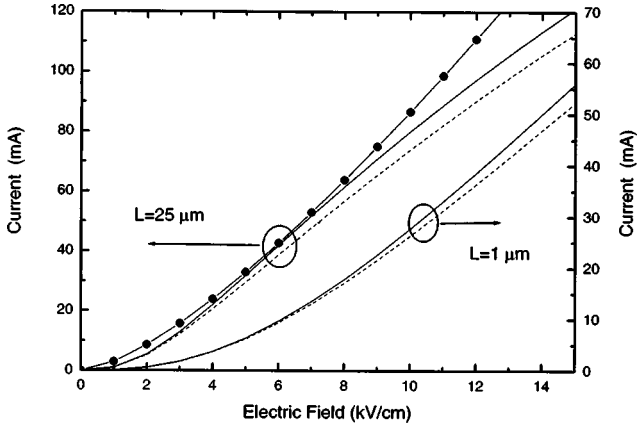

FIG. 3. Separated current reduction due to hot-electron (solid circles) and self-heating effects (see Fig. 2) for $L=1$ μm (right scale) and 25 μm (left scale) for linear (dashed) and nonlinear (solid) cases.

substrate parameters $d=1.5$ mm, $l=300$ μm, and the thermal conductivity of sapphire $\lambda(T)$ given in Ref. 13. As seen from Fig. 2, the computational results are in a good agreement with the experimental data. In particular, at the electric field of 8 kV/cm we obtain the temperature rise $\Delta T=36.2$ K at $P_{\rm dis}=0.63$ W/mm for the channel with $L=1$ μm, and $\Delta T=228.7$ K at $P_{\rm dis}=6.9$ W/mm for $L=25$ μm. The thermal impedances $\theta_1=57.6$ K mm/W and $\theta_{25}=32.9$ K mm/W have been found for $L=1$ and 25 μm, respectively. These values agree well with the thermal impedance obtained for AlGaN/GaN HEMTs grown on sapphire.[7] It also can be estimated that the self-heating effect results in 21.8% and 49.1% of the current reduction for 1 and 25 μm length conducting channels, respectively (Fig. 3). Note that for long channels the self-heating leads to negative differential slope in the $I-E$ curves observed in the experiment.

Since characteristic times determining self-heating kinetics in the epilayer structure and the substrate may differ in several orders of magnitude,[7] pulsed (10^{-6} s) measurements exhibit only partial self-heating in comparison with the steady-state regime. The comparison between the calculated and experimental $I-E$ dependences for the device with $L=25$ μm (Fig. 2) indicates that about 50% of the full (dc) temperature rise is reached in these measurements. Indeed, the time required to establish steady-state thermal process on distance l can be estimated as $\tau=l^2/D$ with D being the thermal diffusivity given as $\lambda/\rho C$, where ρ is the mass density and C is the specific heat capacity. Taking the following numerical values of material parameters for GaN $\rho=6.09$ g/cm^3, $C=0.40$ J/gK, $\lambda=1.3$ W/cm K and for sapphire 3.97 g/cm^3, 0.42 J/gK, 0.33 W/cm K, we get the thermal diffusivity for GaN of 0.53 cm^2/s and for sapphire of 0.2 cm^2/s, respectively. Using these values and $l=1.1$ μm for GaN layer and 300 μm for sapphire substrate, we obtain the corresponding times: $\tau_{\rm GaN}=2.3\times10^{-8}$ s and $\tau_{\rm sapph}=4.5\times10^{-3}$ s. These estimations demonstrate also that hot-electron and self-heating kinetics are well resolved and the concept used of hot carriers in the lattice heated by dissipated power is justified.

In conclusion, we have investigated the 2DEG transport in gateless AlGaN/GaN (TLM) heterostructures grown on sapphire with different lengths of the conducting channel at low and moderate electric fields. The observed strong dependence of the current on the channel length is explained in terms of Joule self-heating effect, which can lead to saturation current or negative differential resistance regimes. The theoretical model used allowed us to discriminate between the current reduction due to hot-electron effect and channel temperature rise caused by the self-heating. The results of pulsed measurements are interpreted in terms of partial self-heating estimated as about 50% of the self-heating under the dc measurements. The results obtained allow us to suggest that to utilize unique properties of group III-nitride heterostructures, including high speed of the channel electrons, it is necessary to further optimize the thermal budget of devices. Such optimization can be achieved in addition to conventional methods[14] by choosing a thinner sapphire substrate, a shorter conducting channel, as well as short-time operating regimes.

This work is supported by the Office of Naval Research under Contract No. N00014-01-1-0828 (monitored by Dr. Colin E. C. Wood). A.E.B. acknowledges Deutsche Forschungsgemeinschaft for a research grant. Contribution of V.A.K. was supported by CRDF Project No. UE-2439-KV-02.

[1] O. Ambacher, B. Foutz, J. Smart, J. R. Shealy, N. J. Weimann, K. Chu, M. Murphy, A. J. Sierakowski, W. J. Schaff, and L. F. Eastman, J. Appl. Phys. **87**, 334 (2000).
[2] S. J. Perton, J. C. Zolper, R. J. Shul, and F. Ren, J. Appl. Phys. **86**, 1 (1999).
[3] E. A. Barry, K. W. Kim, and V. A. Kochelap, Appl. Phys. Lett. **80**, 2317 (2002).
[4] T.-H. Yu and K. F. Brennan, J. Appl. Phys. **89**, 3827 (2001); **91**, 3730 (2002).
[5] B. K. Ridley, J. Appl. Phys. **90**, 6135 (2001).
[6] The range of heating fields can be estimated as $E\gtrsim E_h=u_l/\mu\approx760$ V/cm using the criterion of the absence of electron gas heating for electron scattering by acoustic phonons $(\mu E/u_l)^2\ll1$ with the acoustic-phonon velocity $u_l=7.6\times10^5$ cm/s and the electron mobility $\mu=10^3$ cm^2/V s (300 K). [See T.-H. Yu and K. F. Brennan, J. Appl. Phys. **89**, 3827 (2001); **91**, 3730 (2002).] The consideration of electron-optical phonon scattering yields similar order of magnitude of the heating electric field (of about 1 kV/cm) [E. A. Barry, K. W. Kim, and V. A. Kochelap, Appl. Phys. Lett. **80**, 2317 (2002).]
[7] R. Gaska, A. Osinsky, J. W. Yang, and M. S. Shur, IEEE Electron Device Lett. **19**, 89 (1998).
[8] M. Kuball, J. M. Hayes, M. J. Uren, T. Martin, J. C. H. Birbeck, R. S. Balmer, and B. T. Hughes, IEEE Electron Device Lett. **23**, 7 (2002).
[9] When the thermal conductivity $\lambda(T)$ is a function of temperature, the nonlinear (nl) heat transfer equation and its boundary conditions for temperature $T_{\rm nl}(x,y,z)$ can be reduced to linear (l) form as the constant thermal conductivity $\lambda_0=\lambda(T_0)$ case, $T_l(x,y,z)$, by the Kirchhoff transformation [mathematics in science and engineering, edited by R. Bellman (Academic, New York, 1965), Vol. 18, Chap. 2, pp. 21–23]: $T_l=T_0+(1/\lambda_0)\int_{T_0}^{T_{\rm nl}}\lambda(T')dT'$.
[10] *Mathematics in Science and Engineering*, edited by R. Bellman (Academic, New York, 1965), Vol. 18, Chap. 2, pp. 21–23.
[11] R. Dennemeyer, *Introduction to Partial Differential Equations and Boundary Value Problems* (McGrow-Hill, New York, 1968), Chap. 3, pp. 149–150.
[12] J. R. Shealy, V. Kaper, V. Tilak, T. Prunty, J. A. Smart, B. Green, and L. F. Eastman, J. Phys.: Condens. Matter **14**, 3499 (2002).
[13] D. G. Cahill, S.-M. Lee, and T. I. Selinder, J. Appl. Phys. **83**, 5783 (1998).
[14] P. Horowitz and W. Hill, *The Art of Electronics* (Cambridge University Press, Cambridge, 1989).